AIP | The Journal of Chemical Physics

On the interplay of the potential energy and dipole moment surfaces in controlling the infrared activity of liquid water

Gregory R. Medders and Francesco Paesani

Citation: The Journal of Chemical Physics **142**, 212411 (2015); doi: 10.1063/1.4916629
View online: http://dx.doi.org/10.1063/1.4916629
View Table of Contents: http://scitation.aip.org/content/aip/journal/jcp/142/21?ver=pdfcov
Published by the AIP Publishing

On the interplay of the potential energy and dipole moment surfaces in controlling the infrared activity of liquid water

Gregory R. Medders and Francesco Paesani
Department of Chemistry and Biochemistry, University of California, San Diego, La Jolla, California 92093, USA

(Received 3 February 2015; accepted 16 March 2015; published online 31 March 2015)

Infrared vibrational spectroscopy is a valuable tool for probing molecular structure and dynamics. However, obtaining an unambiguous molecular-level interpretation of the spectral features is made difficult, in part, due to the complex interplay of the dipole moment with the underlying vibrational structure. Here, we disentangle the contributions of the potential energy surface (PES) and dipole moment surface (DMS) to the infrared spectrum of liquid water by examining three classes of models, ranging in complexity from simple point charge models to accurate representations of the many-body interactions. By decoupling the PES from the DMS in the calculation of the infrared spectra, we demonstrate that the PES, by directly modulating the vibrational structure, primarily controls the width and position of the spectroscopic features. Due to the dependence of the molecular dipole moment on the hydration environment, many-body electrostatic effects result in a $\sim$100 cm^{-1} redshift in the peak of the OH stretch band. Interestingly, while an accurate description of many-body collective motion is required to generate the correct (vibrational) structure of the liquid, the infrared intensity in the OH stretching region appears to be a measure of the local structure due to the dominance of the one-body and short-ranged two-body contributions to the total dipole moment. © *2015 AIP Publishing LLC.* [http://dx.doi.org/10.1063/1.4916629]

Often referred to as the "universal solvent," water plays a key role in innumerable chemical phenomena, ranging in scale from hydration of small ions and proteins to the earth's climate.[1] At the most fundamental level, the unique behavior of water centers around its ability to make and break a dynamic network of hydrogen bonds. Because the vibrations of water molecules are sensitive to the surrounding environment, vibrational spectroscopy is a particularly powerful tool for monitoring chemical processes in aqueous systems at the molecular level.[2–11] Due to the chemical complexity of even the most apparently simple aqueous system (i.e., pure liquid water), a molecular interpretation of its corresponding vibrational spectra is often nontrivial.[12] From the theoretical point of view, a consistent interpretation of the vibrational spectra of water has been complicated, in part, by the existence of numerous (both *ab initio* and empirically parametrized) molecular models that can sometimes give conflicting explanations for the same spectroscopic features.[13,14]

To address this issue, we recently introduced a unified methodology for modeling molecular systems, denoted many-body molecular dynamics (MB-MD), which is built entirely upon correlated electronic structure data and includes a quantum-mechanical description of the molecular motion.[15] By construction, MB-MD thus enables "first principles" calculations of structural, thermodynamic, dynamical, and spectroscopic properties of molecular systems from the gas to the condensed phase. Limiting our focus to vibrational spectroscopy, the infrared (IR) spectrum of a generic molecular system can be obtained,[16,17] within the electric dipole approximation and linear response theory, from the Fourier transform of the quantum time autocorrelation function of the system's dipole moment,

$$\alpha(\omega)n(\omega) = \left[\frac{2\omega}{3V\hbar c\epsilon_{\text{vac}}}\right]\tanh\left(\frac{\hbar\omega}{kT}\right)\int_{-\infty}^{\infty} \mathrm{d}t\, \mathrm{e}^{-i\omega t}\langle\boldsymbol{\mu}(0)\boldsymbol{\mu}(t)\rangle. \tag{1}$$

Through the MB-MD methodology, empirical parameter-free representations of the two properties that are required for the calculation of IR vibrational spectra, the multidimensional potential energy surface (PES) and dipole moment surface (DMS), are independently derived from large datasets of correlated electronic structure calculations.[15] While dynamical effects, such as motional narrowing, play an important role in determining the final line shapes,[18–20] from a static perspective, the IR spectrum can be related to the frequencies of the vibrational modes determined by the multidimensional potential energy surface weighted by the associated squared transition dipoles. In this contribution, we seek to understand the roles of both PES and DMS in determining the IR activity of liquid water by investigating the properties of three different molecular models that have been previously applied to the study of IR spectra.

The first model, q-TIP4P/f, is a flexible point charge force field that was empirically parametrized to reproduce thermodynamic and dynamical properties of bulk water.[21] q-TIP4P/f employs fixed point charges located on the hydrogen atoms and a fictitious "M-site" located along the HOH bisector. Fixed charge models are, however, unable to correctly describe the geometry dependence of the molecular dipole of water, an effect which is important for reproducing the correct IR spectral intensities of water.[19,22] Furthermore, such models predict that molecules with the same internal geometry but which reside

in different hydration environments have the same dipole moments, which limits the ability of such models to reproduce the IR absorption intensities.[23,24] Polarizable force fields, on the other hand, allow the molecular charge distributions to adapt to the surrounding electrostatic environments.[25] As a representative example of polarizable force fields, we consider the TTM3-F model,[26] which has been extensively used in simulations of vibrational spectra.[27–29] TTM3-F was fitted to a relatively small set of *ab initio* data and employs "Thole type" damped point polarizable dipoles to recover induced dipole effects.[30] Though its associated molecular DMS is based on an accurate fit to correlated electronic structure data,[31] the TTM3-F model empirically adjusts the gas phase dipole moment to generate an effective DMS that partially accounts for environmental effects in the condensed phase.[26] This is similar to strategies employed in other polarizable models, where the charges were modified to reproduced spectroscopic features.[32,33]

The final model considered here is the many-body MB-pol PES and the associated MB-μ DMS, recently developed by us.[15] Both MB-pol PES[34–36] and MB-μ DMS[15] were independently developed by using the many-body expansion of the interaction energy (and its derivatives with respect to electric fields),

$$E_N(x_1,\ldots,x_N) = \sum_a V^{(1B)}(x_a) + \sum_{a<b} V^{(2B)}(x_a,x_b) + \cdots + V^{(NB)}(x_1,\ldots,x_N). \quad (2)$$

Equation (2) is a rigorous representation of the total interaction energy of a generic N-molecule system which is expressed as a sum of one-body (1B) monomer distortion energies and two-body (2B) pairwise interactions, up to N-body interactions.[37] The MB-pol PES relies on explicit fits to a large number of correlated electronic structure data for the 1B, 2B, and 3B interactions, while including all higher-order terms in Eq. (2) through many-body induction.[34,38] The even more rapid convergence of the many-body expansions for the water dipole moment and polarizability (established in Ref. 39) allowed us to introduce highly accurate multidimensional representations for these properties (called MB-μ and MB-α, respectively). These many-body representations describe the dipole moment and polarizability of an N-molecule water system in terms of explicit 1B and 2B contributions derived from correlated electronic structure data, with all higher-order interactions being included through many-body induction.[15] The MB-μ and MB-α surfaces were employed in adiabatic centroid molecular dynamics (CMD)[40,41] simulations carried out with the MB-pol PES to model the infrared and Raman spectra of liquid water at ambient conditions.[15] Detailed comparisons with experimental measurements and electronic structure data obtained at the MP2 level demonstrated the accuracy of the MB-MD methodology in reproducing both positions and shapes of all spectral features. The analysis of the stretching band calculated for pure H_2O and a dilute mixture of HOD in H_2O also highlighted some differences in the low-frequency portion of the band (~3000-3250 cm^{-1}) compared to the experimental line shape. We refer the reader to Ref. 15 for a discussion of possible sources for this missing intensity.

In this contribution, following Ref. 15, the calculation of the relevant quantum dipole autocorrelation function (Eq. (1)) was carried out within the CMD formalism, which has been shown to provide an approximate yet accurate description of several quantum dynamical properties of liquid water at ambient conditions.[42,43] Specifically, for each model PES described above (q-TIP4P/f, TTM3-F, and MB-pol), path-integral molecular dynamics (PIMD) simulations[44] were initially performed in the NVT ensemble for systems containing 216 molecules at 298.15 K and experimental density. Using 10 different initial conditions obtained from the PIMD simulations, 27 ps adiabatic CMD simulations were then performed in the normal-mode representation. The quantum partition function was discretized using 32 quasiparticles or "beads," and an adiabaticity parameter $\gamma = 0.1$ was used to guarantee a sufficient decoupling between the dynamics of the centroid variables and the non-zero frequency normal modes.[41,43] A time step of 0.02 fs was used to ensure energy conservation and the dynamical trajectories were saved every 2 fs to enable the calculation of the quantum dipole autocorrelation function required by Eq. (1). The "time-reversible always stable predictor-corrector" method was used with fourth order extrapolation in the predictor to obtain the induced dipoles.[45]

We begin the analysis of the infrared spectra of water by briefly summarizing the main spectroscopic features of interest: (1) a small shoulder at ~180 cm^{-1} associated with the hydrogen bond stretch corresponding to hindered translations of molecules within the liquid; (2) a broad librational band at <1000 cm^{-1} associated with hindered reorientations of molecules within the hydrogen bonding network; (3) a peak at ~1650 cm^{-1}, associated with the HOH bending vibration; (4) a small, broad feature near ~2250 cm^{-1} corresponding to the combination band of the bending vibrations with librations; and (5) a broad feature at 3000-3750 cm^{-1}, corresponding to the OH stretching vibrations. Although the details of these features will be discussed in depth later, it is useful to make some general comments about the performance of the three different water models. As was mentioned earlier, because the q-TIP4P/f molecular dipole moment does not respond to the fluctuating electric field of the surrounding environment, it is to be expected that the infrared intensities predicted by q-TIP4P/f differ significantly from experiment. Despite the fact that the q-TIP4P/f bend and stretch features are thus predicted to have nearly the same intensity, the overall position of these features are in reasonably good agreement with experiment as a result of the empirical parameterization. TTM3-F, which includes induced dipole effects, more accurately predicts the relative intensities for the bending and stretching bands. However, while position and width of the classical TTM3-F stretch and bend features were shown to be in good agreement with experiment,[26] inclusion of nuclear quantum effects results in a significant redshift of both bands.[27] The bending and stretching spectral features predicted by the MB-pol PES in combination with the MB-μ DMS are in good agreement with experiment in terms of their positions, shapes, and intensities, although, as discussed in Ref. 15, the intensity is underestimated on the red portion of the OH stretching band.

While Figure 1 is sufficient to make general statements about the accuracy of the three different water models, it does

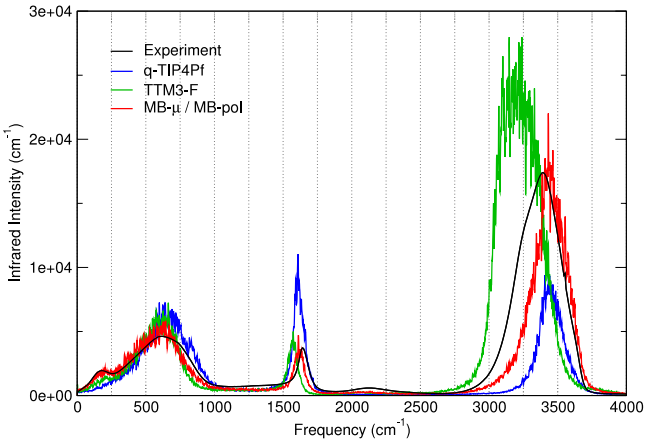

FIG. 1. Infrared spectra of liquid water predicted by the q-TIP4P/f (blue), TTM3-F (green), and MB-μ/MB-pol (red) models. The spectra were calculated through Eq. (1), with the ensemble average obtained through CMD simulations performed at 298.15 K. The experimental data (black) are adapted from Ref. 46.

little to explain what physical aspects of a model make it more or less accurate. Since the infrared activity is related to both the vibrational structure of the energy landscape and the dipole derivatives along those vibrational coordinates, we attempt to better assess the accuracy of each model by decoupling the effects associated with the corresponding PES and DMS. For this purpose, the dynamical trajectories obtained from the CMD simulations carried out with each model PES are combined in turn with the DMSs associated with the other models. This results in 9 different quantum dipole autocorrelation functions, leading to the 9 IR spectra shown in Figure 2, each of which is labeled according to the notation "DMS/PES."

The hydrogen bond stretch at ~180 cm^{-1} is a key feature to highlight polarization effects on the IR spectra. While all three model PESs are capable of describing hindered translations between hydrogen bonded molecules, the q-TIP4P/f simple point charge representation of the dipole moment, which is independent of the surrounding chemical environment, necessarily generates no IR signal from this purely translational motion.[23] This effect can be clearly seen in the top row of Figure 2 (corresponding to the q-TIP4P/f, TTM3-F, and MB-pol CMD trajectories combined with the q-TIP4P/f DMS), where no distinct feature corresponding to the hydrogen bond stretch can be identified in the region between 0 and 250 cm^{-1}. When the CMD trajectories are combined with the TTM3-F DMS (middle row of Figure 2), some enhancement in the 0-250 cm^{-1} region is observed, particularly in the case of MB-pol trajectories (panel (f)), although the hydrogen bond stretch is still not well resolved with any of the combinations of the TTM3-F DMS with the three PESs. On the other hand, the

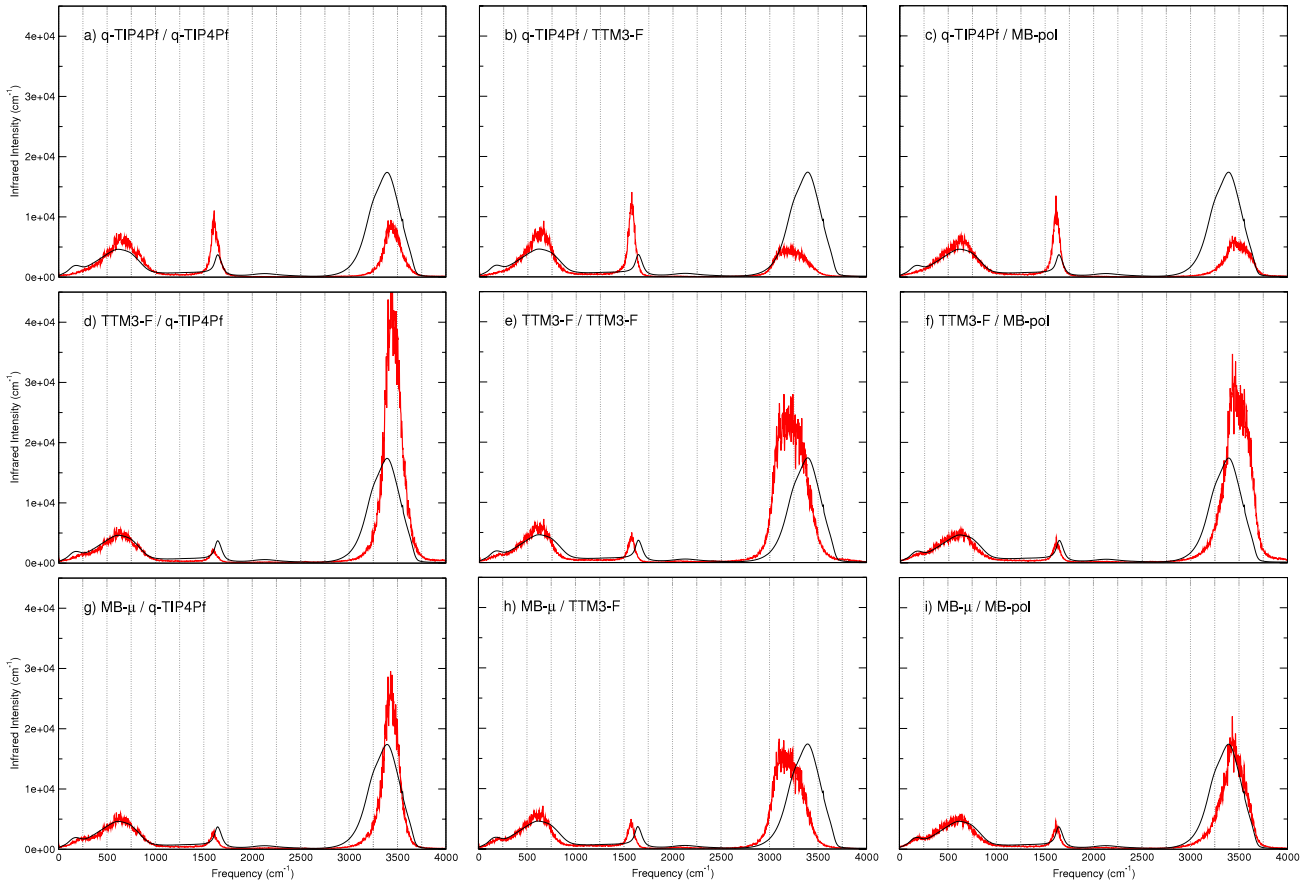

FIG. 2. Infrared spectra obtained from different combinations of PES and DMS. The panels are labeled using the notation "DMS/PES." Each row thus displays the IR spectra calculated with the same model DMS combined with CMD trajectories obtained with the three model PESs. Analogously, each column displays the IR spectra calculated with the different model DMSs combined with CMD trajectories obtained with the same model PES. For example, in panel (d), the IR spectrum is calculated using the DMS of the TTM3-F model combined with the CMD trajectory obtained with the q-TIP4P/f model. In each panel, the experimental infrared spectrum is shown in black.

hydrogen bond stretch feature is found to be in good agreement with experiment when the MB-μ DMS is combined with the CMD trajectories performed with the MB-pol PES.

The different shapes of the hydrogen bond stretch features of the MB-pol PES identified in panels (f) and (i) can be traced back to (at least) two main differences between the MB-μ and TTM3-F DMSs. First, the TTM3-F DMS, which has only a single (isotropic) polarizable site on each molecule, is unable to completely capture the anisotropy of the induced dipole along the hydrogen bond stretching coordinate. Second, the TTM3-F DMS only accounts for induced dipoles, neglecting charge transfer effects which have been proposed to be an important source of spectral intensity for the hydrogen bond stretching vibration in Raman calculations.[47] The MB-μ DMS, on the other hand, includes both the anisotropy of the 2B induced dipole and all charge transfer effects, which are accurately modeled at the MP2 level. Unfortunately, a precise decomposition of the different electronic contributions to the IR intensity associated with the hydrogen bond stretching vibration cannot be obtained through the analysis of the TTM3-F and MB-μ DMSs since such analysis requires models that are capable of accurately and explicitly distinguishing charge transfer from induction. It can also be noted that the hydrogen bond stretch of both the q-TIP4P/f and TTM3-F PESs is blue shifted (by 80 and 30 cm^{-1}, respectively) relative to experiment when calculated using the MB-μ DMS, indicating that the hydrogen bonds in these models are possibly too strong. The librational band is well described by both q-TIP4P/f and MB-pol PESs when the accurate many-body MB-μ DMS is used (panels (g) and (i)), while it appears to be slightly too narrow in the case of the TTM3-F PES (panel (h)). By contrast, both q-TIP4P/f and TTM3-F DMSs tend to overestimate the intensity of the librational band, particularly near the maximum at ~600 cm^{-1}.

Examining the spectral features associated with the intramolecular bending and stretching vibrations, it is clear that the energy landscape defined by the individual PESs primarily controls the position of these two bands. To understand the spuriously similar intensity of the spectral features associated with the bending and stretching vibrations in the q-TIP4P/f spectrum shown in Figure 1, the MB-μ DMS is applied to the q-TIP4P/f PES in panel (g) of Figure 2. The overestimated intensity of the OH stretch band when using an accurate DMS indicates that the q-TIP4P/f PES may not be capable of accurately describing the dependence on the intramolecular stretching vibrations on strength of the intermolecular hydrogen bonds. In particular, the high infrared intensity of the OH stretching band may suggest that the underlying frequency distribution of the q-TIP4P/f OH stretch is too narrow, implying that the q-TIP4P/f OH oscillators either sample a restricted range of hydrogen bonding environments or that the two OH oscillators of each molecule do not sufficiently couple to one another to acquire partial symmetric/asymmetric splitting.[48]

At the same time, the q-TIP4P/f DMS also suffers from deficiencies. An accurate 1B representation of the DMS should have a low intensity in the OH stretching region (see Figure 3). Despite the fact that it uses a purely 1B representation of the DMS, the q-TIP4P/f DMS applied to the MB-pol PES results in an artificially enhanced height of the OH stretch band. The electrostatic origin of this spuriously large intensity can be more clearly seen in the bending region. Regardless of which PES is used, the q-TIP4P/f DMS always predicts a high bend intensity. However, applying either the TTM3-F or the MB-μ DMS to the q-TIP4P/f PES brings the bend intensity into reasonable agreement with experiment. This high intensity caused by the q-TIP4P/f DMS would likely be observed in all fixed point charge models of water which represent the enhanced condensed-phase dipole through the use of artificially large effective charges. Through the analysis of the q-TIP4P/f infrared line shape, it can thus be seen that decoupling the influence of the PES from the DMS in the calculation of infrared spectra provides specific insights that are useful to assess the ability of a model to correctly reproduce the underlying physics.

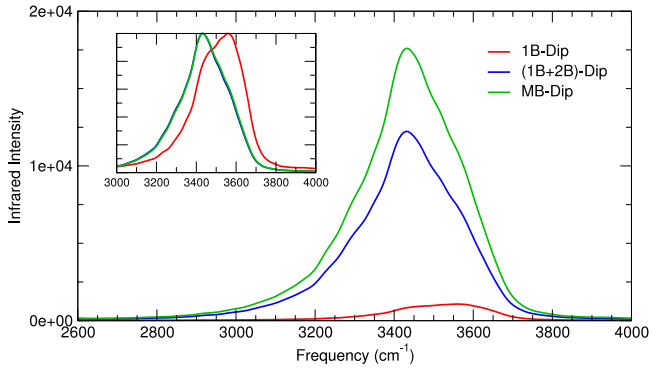

FIG. 3. Decomposition of the IR spectrum obtained from CMD trajectories with the MB-pol PES in terms of the many-body components of the MB-μ DMS. 1B-Dip indicates that the one-body (gas-phase monomer) dipoles were used to calculate the dipole of the molecules sampled along the MB-pol CMD trajectories, from which the IR spectrum was calculated. (1B + 2B)-Dip indicates that short-ranged two-body dipoles were used in addition to the one-body dipoles. MB-Dip is the full MB-μ many-body dipole. The inset shows each curve normalized to its corresponding maximum. The spectra were smoothed to facilitate the comparison between the line shapes obtained using the different approximations.

To further investigate the role of the DMS in determining the position and shape of the OH stretching band, we performed a many-body decomposition of the dipole moment using the MB-μ DMS. Specifically, for the set of CMD trajectories carried out with the MB-pol PES, the total dipole moment was calculated according to three different approximations: the 1B approximation (i.e., only including all molecular gas-phase dipoles in the geometry of the liquid), the 1B + 2B approximation (i.e., adding all short-ranged pairwise interaction-induced dipoles to the 1B total dipole moment), and the MB approximation using with the full MB-μ DMS (i.e., including 3B and higher-order induced dipoles to the 1B + 2B total dipole). Focusing on the OH stretch band shown in Figure 3, the 1B dipole approximation predicts a very weak OH stretch intensity. This result is not unexpected since the average dipole moment of a water molecule increases significantly upon solvation relative to its gas-phase value. Therefore, neglecting all solvation-induced effects, the 1B approximation consistently underestimates the infrared intensity. Inclusion of the short-ranged (i.e., for pairs of molecules with an oxygen-oxygen separation of <3.7 Å) pair-wise interaction-induced dipoles results in a substantial increase in the OH stretch

intensity, with the full many-body dipole contributing a slight additional enhancement and bringing the total intensity into good agreement with experiment. The many-body dipoles also have an additional effect on the position of the OH stretching band as demonstrated in the inset of Figure 3 by normalizing 1B, 1B + 2B, and MB bands to the corresponding maxima. While the 2B dipole enhances the overall intensity, it does so preferentially for OH stretches in more strongly H-bonded configurations. In general terms, this is consistent with the picture that the magnitude of the change of the dipole moment with respect to a vibrational coordinate is much larger when the OH is vibrating into a nearby H-bond acceptor relative to its rate of change in a weak or broken H-bond configuration. The many-body analysis shown in Figure 3 thus demonstrates that this "non-Condon" effect plays an important role at the 2B dipole level,[49] with all higher-order induced dipoles having a negligible impact on the position of the OH stretching band.

It is often assumed that the underlying multidimensional PES is primarily responsible for the position (and, to a large extent, the shape) of the infrared spectrum of liquid water. There are, however, interesting cases for which this first order assumption breaks down, namely, where there exists a non-uniform distribution of dipole derivative magnitudes that can result in a preferential enhancement of some portions of the line shape with respect to others. Here, we illustrated an excellent example of this through the analysis of the hydrogen bond stretch feature at ~180 cm^{-1}. While non-existent in intensity for models which have no induced, many-body dipoles, the peak appears (although is not well-resolved) for a non-polarizable PES when combined with a many-body DMS. Ultimately, an accurate representation of both the potential energy surface and the dipole moment surface is necessary to obtain good agreement with the experimental infrared spectrum of liquid water. By examining the detailed many-body contributions of the dipole to the infrared spectrum, the line shape of the OH band is shown to be well described through a sum of molecular dipoles and short-ranged two-body dipoles. This supports an interpretation of the IR intensity of the OH band of liquid water as a probe of the local hydration environment. A question that remains to be addressed is the extent to which the underlying frequency distribution is affected by delocalized collective vibrations.

This research was supported by the National Science Foundation Center for Chemical Innovation "Center for Aerosol Impacts on Climate and the Environment" (Grant No. CHE-1305427). This work used the Extreme Science and Engineering Discovery Environment (XSEDE), which is supported by the National Science Foundation Grant No. ACI-1053575 (Allocation No. TG-CHE110009). G.R.M. acknowledges the Department of Education for support through the GAANN fellowship program. We thank Prof. Andrei Tokmakoff and Prof. Peter Hamm for helpful discussions about collective motions in infrared spectroscopy.

[1]Y. Maréchal, *The Hydrogen Bond and the Water Molecule: The Physics and Chemistry of Water, Aqueous and Bio-Media* (Elsevier, Amsterdam, 2006).

[2]A. P. Ault, T. L. Guasco, O. S. Ryder, J. Baltrusaitis, L. A. Cuadra-Rodriguez, D. B. Collins, M. J. Ruppel, T. H. Bertram, K. A. Prather, and V. H. Grassian, "Inside versus outside: Ion redistribution in nitric acid reacted sea spray aerosol particles as determined by single particle analysis," J. Am. Chem. Soc. **135**, 14528–14531 (2013).

[3]F. N. Keutsch and R. J. Saykally, "Water clusters: Untangling the mysteries of the liquid, one molecule at a time," Proc. Natl. Acad. Sci. U. S. A. **98**, 10533–10540 (2001).

[4]M. D. Fayer and N. E. Levinger, "Analysis of water in confined geometries and at interfaces," Annu. Rev. Anal. Chem. **3**, 89–107 (2010).

[5]A. M. Jubb, W. Hua, and H. C. Allen, "Environmental chemistry at vapor/water interfaces: Insights from vibrational sum frequency generation spectroscopy," Annu. Rev. Phys. Chem. **63**, 107–130 (2012).

[6]S. Bourrelly, B. Moulin, A. Rivera, G. Maurin, S. Devautour-Vinot, C. Serre, T. Devic, P. Horcajada, A. Vimont, G. Clet, M. Daturi, J.-C. Lavalley, S. Loera-Serna, R. Denoyel, P. L. Llewellyn, and G. Férey, "Explanation of the adsorption of polar vapors in the highly flexible metal organic framework MIL-53(Cr)," J. Am. Chem. Soc. **132**, 9488–9498 (2010).

[7]S. Horvath, A. B. McCoy, B. M. Elliott, G. H. Weddle, J. R. Roscioli, and M. A. Johnson, "Anharmonicities and isotopic effects in the vibrational spectra of X-·H2O, ·HDO, and ·D2O[X = Cl, Br, and I] binary complexes," J. Phys. Chem. A **114**, 1556–1568 (2010).

[8]F. Perakis, J. a. Borek, and P. Hamm, "Three-dimensional infrared spectroscopy of isotope-diluted ice Ih," J. Chem. Phys. **139**, 014501 (2013).

[9]G. R. Medders and F. Paesani, "Water dynamics in metal-organic frameworks: Effects of heterogeneous confinement predicted by computational spectroscopy," J. Phys. Chem. Lett. **5**, 2897–2902 (2014).

[10]L. Piatkowski, Z. Zhang, E. H. G. Backus, H. J. Bakker, and M. Bonn, "Extreme surface propensity of halide ions in water," Nat. Commun. **5**, 4083 (2014).

[11]Z. L. Terranova and S. A. Corcelli, "Molecular dynamics investigation of the vibrational spectroscopy of isolated water in an ionic liquid," J. Phys. Chem. B **118**, 8264–8272 (2014).

[12]H. J. Bakker and J. L. Skinner, "Vibrational spectroscopy as a probe of structure and dynamics in liquid water," Chem. Rev. **110**, 1498–1517 (2010).

[13]S. Nihonyanagi, T. Ishiyama, T. Lee, S. Yamaguchi, M. Bonn, A. Morita, and T. Tahara, "Unified molecular view of the air/water interface based on experimental and theoretical χ ((2)) spectra of an isotopically diluted water surface," J. Am. Chem. Soc. **133**, 16875–16880 (2011).

[14]J. L. Skinner, P. A. Pieniazek, and S. M. Gruenbaum, "Vibrational spectroscopy of water at interfaces," Acc. Chem. Res. **45**, 93–100 (2012).

[15]G. R. Medders and F. Paesani, "Infrared and Raman spectroscopy of liquid water through first principles many-body molecular dynamics," J. Chem. Theory Comput. **11**, 1145–1154 (2015).

[16]S. Mukamel, *Principles of Nonlinear Optical Spectroscopy* (Oxford University Press, Oxford, 1995).

[17]A. Nitzan, *Chemical Dynamics in Condensed Phases* (Oxford University Press, 2006).

[18]R. Kubo, "A stochastic theory of line shape," Adv. Chem. Phys. **15**, 101 (1969).

[19]H. Ahlborn, X. Ji, B. Space, and P. B. Moore, "A combined instantaneous normal mode and time correlation function description of the infrared vibrational spectrum of ambient water," J. Chem. Phys. **111**, 10622 (1999).

[20]J. L. Skinner, B. M. Auer, and Y.-s. Lin, "Vibrational line shapes, spectral diffusion, and hydrogen bonding in liquid water," Adv. Chem. Phys. **142**, 59–103 (2009).

[21]S. Habershon, T. E. Markland, and D. E. Manolopoulos, "Competing quantum effects in the dynamics of a flexible water model," J. Chem. Phys. **131**, 024501 (2009).

[22]C. J. Burnham and S. S. Xantheas, "Development of transferable interaction models for water. IV. A flexible, all-atom polarizable potential (TTM2-F) based on geometry dependent charges derived from an *ab initio* monomer dipole moment surface," J. Chem. Phys. **116**, 5115 (2002).

[23]S. Iuchi, A. Morita, and S. Kato, "Molecular dynamics simulation with the charge response kernel: Vibrational spectra of liquid water and n -methylacetamide in aqueous solution," J. Phys. Chem. B **106**, 3466–3476 (2002).

[24]T. Ishiyama and A. Morita, "Analysis of anisotropic local field in sum frequency generation spectroscopy with the charge response kernel water model," J. Chem. Phys. **131**, 244714 (2009).

[25]P. Barnes, J. L. Finney, J. D. Nicholas, and J. E. Quinn, "Cooperative effects in simulated water," Nature **282**, 459–464 (1979).

[26]G. S. Fanourgakis and S. S. Xantheas, "Development of transferable interaction potentials for water. V. Extension of the flexible, polarizable, Thole-type model potential (TTM3-F, v. 3.0) to describe the vibrational spectra of water clusters and liquid water," J. Chem. Phys. **128**, 074506 (2008).
[27]S. Habershon, G. S. Fanourgakis, and D. E. Manolopoulos, "Comparison of path integral molecular dynamics methods for the infrared absorption spectrum of liquid water," J. Chem. Phys. **129**, 074501 (2008).
[28]F. Paesani, S. S. Xantheas, and G. A. Voth, "Infrared spectroscopy and hydrogen-bond dynamics of liquid water from centroid molecular dynamics with an ab initio-based force field," J. Phys. Chem. B **113**, 13118–13130 (2009).
[29]F. Paesani, "Temperature-dependent infrared spectroscopy of water from a first-principles approach," J. Phys. Chem. A **115**, 6861–6871 (2011).
[30]B. T. Thole, "Molecular polarizabilities calculated with a modified dipole interaction," Chem. Phys. **59**, 341–350 (1981).
[31]H. Partridge and D. W. Schwenke, "The determination of an accurate isotope dependent potential energy surface for water from extensive *ab initio* calculations and experimental data," J. Chem. Phys. **106**, 4618 (1997).
[32]P. K. Mankoo and T. Keyes, "POLIR: Polarizable, flexible, transferable water potential optimized for IR spectroscopy," J. Chem. Phys. **129**, 034504 (2008).
[33]T. Hasegawa and Y. Tanimura, "A polarizable water model for intramolecular and intermolecular vibrational spectroscopies," J. Phys. Chem. B **115**, 5545–5553 (2011).
[34]V. Babin, C. Leforestier, and F. Paesani, "Development of a first principles water potential with flexible monomers: Dimer potential energy surface, VRT spectrum, and second virial coefficient," J. Chem. Theory Comput. **9**, 5395–5403 (2013).
[35]V. Babin, G. R. Medders, and F. Paesani, "Development of a first principles water potential with flexible monomers. II: Trimer potential energy surface, third virial coefficient, and small clusters," J. Chem. Theory Comput. **10**, 1599–1607 (2014).
[36]G. R. Medders, V. Babin, and F. Paesani, "Development of a first-principles water potential with flexible monomers. III. Liquid phase properties," J. Chem. Theory Comput. **10**, 2906–2910 (2014).
[37]G. R. Medders, V. Babin, and F. Paesani, "A critical assessment of two-body and three-body interactions in water," J. Chem. Theory Comput. **9**, 1103–1114 (2013).
[38]C. J. Burnham, D. J. Anick, P. K. Mankoo, and G. F. Reiter, "The vibrational proton potential in bulk liquid water and ice," J. Chem. Phys. **128**, 154519 (2008).
[39]G. R. Medders and F. Paesani, "Many-body convergence of the electrostatic properties of water," J. Chem. Theory Comput. **9**, 4844–4852 (2013).
[40]J. Cao and G. A. Voth, "The formulation of quantum statistical mechanics based on the Feynman path centroid density. II. Dynamical properties," J. Chem. Phys. **100**, 5106 (1994).
[41]T. D. Hone and G. A. Voth, "A centroid molecular dynamics study of liquid para-hydrogen and ortho-deuterium," J. Chem. Phys. **121**, 6412 (2004).
[42]F. Paesani and G. A. Voth, "A quantitative assessment of the accuracy of centroid molecular dynamics for the calculation of the infrared spectrum of liquid water," J. Chem. Phys. **132**, 014105 (2010).
[43]M. Rossi, H. Liu, F. Paesani, J. Bowman, and M. Ceriotti, "Communication: On the consistency of approximate quantum dynamics simulation methods for vibrational spectra in the condensed phase," J. Chem. Phys. **141**, 181101 (2014).
[44]M. E. Tuckerman, "Path integration via molecular dynamics," in *Quantum Simulations of Complex Many-Body Systems: From Theory to Algorithms*, edited by J. Grotendorst, D. Marx, and A. Muramatsu (John von Neumann Institute for Computing, Julich, 2002), Vol. 10, pp. 269–298.
[45]J. Kolafa, "Time-reversible always stable predictor–corrector method for molecular dynamics of polarizable molecules," J. Comput. Chem. **25**, 335–342 (2004).
[46]J. E. Bertie and Z. Lan, "Infrared intensities of liquids XX : The intensity of the O H stretching band of liquid water revisited , and the best current values of the optical constants of H20 (I) at 25 C between 15 , 000 and 1 cm -1," Appl. Spectrosc. **50**, 1047–1057 (1996).
[47]Q. Wan, L. Spanu, G. A. Galli, and F. Gygi, "Raman spectra of liquid water from *ab initio* molecular dynamics: Vibrational signatures of charge fluctuations in the hydrogen bond network," J. Chem. Theory Comput. **9**, 4124–4130 (2013).
[48]C. Zhang, R. Z. Khaliullin, D. Bovi, L. Guidoni, and T. D. Kühne, "Vibrational signature of water molecules in asymmetric hydrogen bonding environments," J. Phys. Chem. Lett. **4**, 3245–3250 (2013).
[49]J. R. Schmidt, S. A. Corcelli, and J. L. Skinner, "Pronounced non-Condon effects in the ultrafast infrared spectroscopy of water," J. Chem. Phys. **123**, 044513 (2005).